NANO LETTERS

2007
Vol. 7, No. 1
75−80

The SERS and TERS Effects Obtained by Gold Droplets on Top of Si Nanowires

M. Becker,*,† V. Sivakov,‡,§ G. Andrä,§ R. Geiger,|| J. Schreiber,⊥ S. Hoffmann,# J. Michler,# A. P. Milenin,‡ P. Werner,‡ and S. H. Christiansen†,‡

Martin-Luther-University Halle-Wittenberg, Hoher Weg 8, 06109 Halle, Germany, Max-Planck-Institute of Microstructure Physics, Weinberg 2, 06120 Halle, Germany, Institute for Physical Hightechnology e.V., Albert-Einstein strasse 9, 07745 Jena, Germany, Horiba Jobin Yvon GmbH, Neuhofstrasse 9, 64625 Bensheim, Germany, Horiba Jobin Yvon SAS, rue de Lille 231, 59650 Villeneuve d'Ascq, France, EMPA, Swiss Federal Laboratories for Materials Testing and Research, Materials and Nanomechanics Laboratory, Feuerwerkerstrasse 39, CH-3602 Thun, Switzerland

Received September 8, 2006; Revised Manuscript Received December 4, 2006

ABSTRACT

We show that hemispherical gold droplets on top of silicon nanowires when grown by the vapor−liquid−solid (VLS) mechanism, can produce a significant enhancement of Raman scattered signals. Signal enhancement for a few or even just single gold droplets is demonstrated by analyzing the enhanced Raman signature of malachite green molecules. For this experiment, trenches (∼800 nm wide) were etched in a silicon-on-insulator (SOI) wafer along ⟨110⟩ crystallographic directions that constitute sidewalls ({110} surfaces) suitable for the growth of silicon nanowires in ⟨111⟩ directions with the intention that the gold droplets on the silicon nanowires can meet somewhere in the trench when growth time is carefully selected. Another way to realize gold nanostructures in close vicinity is to attach a silicon nanowire with a gold droplet onto an atomic force microscopy (AFM) tip and to bring this tip toward another gold-coated AFM tip where malachite green molecules were deposited prior to the measurements. In both experiments, signal enhancement of characteristic Raman bands of malachite green molecules was observed. This indicates that silicon nanowires with gold droplets atop can act as efficient probes for tip-enhanced Raman spectroscopy (TERS). In our article, we show that a nanowire TERS probe can be fabricated by welding nanowires with gold droplets to AFM tips in a scanning electron microscope (SEM). TERS tips made from nanowires could improve the spatial resolution of Raman spectroscopy so that measurements on the nanometer scale are possible.

1. Introduction. Surface-enhanced Raman spectroscopy (SERS) is now in use for almost three decades[1−3] to detect Raman signals of low molecule concentrations that cannot be detected by conventional Raman spectroscopy. To exploit the SERS effect, colloid solutions containing nanosized noble metal particles[4] or substrates with noble metal nanoparticles on their surfaces are usually used.[5,6] However, these particles are usually inhomogeneous in size and shape, e.g., the small gold particles on a Si substrate, which are produced by annealing a thin (few nanometer thick) gold layer that decomposes into nanoscale gold droplets, show a broad size distribution and exhibit a lens shape[7] instead of, for signal enhancement, the more desirable hemispherical or rodlike shape.[8] Moreover, these experiments cannot provide signal enhancement at predefined locations on a sample where spatial resolution at the nanometer scale is required. These inherent disadvantages of the conventional SERS substrates are circumvented by using the hemispherical gold droplets atop silicon nanowires as they occur during the (VLS) growth[9,10] of semiconductor nanowires (NWs). Also, welding a silicon nanowire with a gold droplet atop onto an AFM tip yields a probe for tip-enhanced Raman spectroscopy (TERS), similar to the tip presented in ref 11. In our paper, we show that silicon nanowires with hemispherical gold droplets atop generate the SERS effect and that they are in addition well suited for TERS measurements, thereby giving Raman spectroscopy a spatial resolution on the nanometer scale.[12−15]

2. Silicon Nanowires: Growth and Morphology. For our SERS and TERS measurements, we used silicon nanowires that were grown by physical vapor deposition techniques such as electron beam evaporation (EBE) or molecular

* Corresponding author. E-mail: mbecker@mpi-halle.mpg.de.
† Martin-Luther-University Halle-Wittenberg.
‡ Max-Planck-Institute of Microstructure Physics.
§ Institute for Physical Hightechnology e.V.
|| Horiba Jobin Yvon GmbH.
⊥ Horiba Jobin Yvon SAS.
EMPA, Swiss Federal Laboratories for Materials Testing and Research.

10.1021/nl0621286 CCC: $37.00
Published on Web 12/21/2006

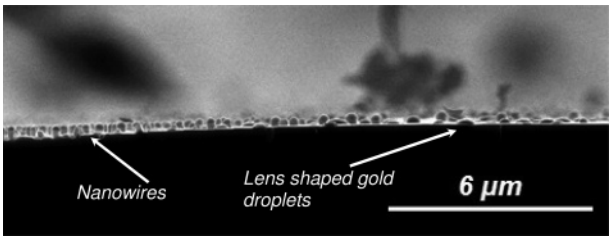

Figure 1. Cross-sectional SEM micrograph of an assembly of nanowires (left side of the micrograph) grown by EBE at 700 °C with 1.2 nm sputtered Au on a p-Si(111) substrate for 15 min. Lens-shaped gold droplets (right side of the micrograph) formed under the clamp of the sample holder upon annealing, however, without exposure to evaporated silicon. The radii of curvature of the gold droplets atop the nanowires are ∼5−10 times smaller than those of the gold particles on the substrate surface.

beam epitaxy (MBE), utilizing the VLS growth mechanism. Both methods give comparable results in terms of nanowire growth morphologies, although vacuum conditions are quite severe in the case of MBE, where ultrahigh vacuum is required. EBE nanowires grow from evaporated silicon atoms, obtained by directing an electron beam on a high resistivity silicon target. For evaporation, beam currents of 80 mA are used. The silicon atoms from the vapor are incorporated at growth temperature in a liquid gold (Au) droplet on the silicon substrate surface that catalyzes the one-dimensional NW growth. The gold droplets form upon annealing a 0.5−2 nm Au layer above the eutectic temperature of the Au−Si alloy at 373 °C[16] on silicon wafers. Supersaturation of the gold droplet with silicon yields the NW growth. During growth, the liquid gold droplets stay on top of the NWs and, upon solidification, gold hemispheres form in a self-controlled manner. The diameter of the NWs is initially determined by the size of the gold droplet on the silicon substrate, which itself depends on the thickness of the sputtered Au starting layer, annealing times, and temperatures. Effects like Ostwald ripening[17,18] are responsible for thick NWs to grow thicker and thin NWs to become thinner, together with the change of the size of the gold droplets. For a short growth time (5−15 min) in EBE at high emission currents (e.g., 80 mA), the NW diameters show a narrow size distribution, and although NWs are still short, they already have the hemispherical gold droplets atop after solidification. Figure 1 shows a cross-sectional SEM micrograph of an assembly of silicon NWs (left side of the micrograph) grown by EBE on a p-Si(111) substrate at 700 °C. The initial gold layer was 1.2 nm thick. The right side of the micrograph shows the lens-shaped gold droplets formed at 700 °C as well. Silicon NWs did not grow on the right side, as this area was masked off from the Si vapor by the clamp of the sample holder. The silicon NWs shown in Figure 1 (left side) have diameters between ∼150 and ∼300 nm. The radii of curvature of the gold droplets located atop the Si nanowires are a factor of ∼5−10 smaller than those of the lens-shaped gold droplets on the substrate surface (right side). This renders the gold droplets atop the silicon NWs to be better suited for SERS measurements than those directly formed on the substrate surface because they suggest larger enhancement due to geometrical reasons.[8]

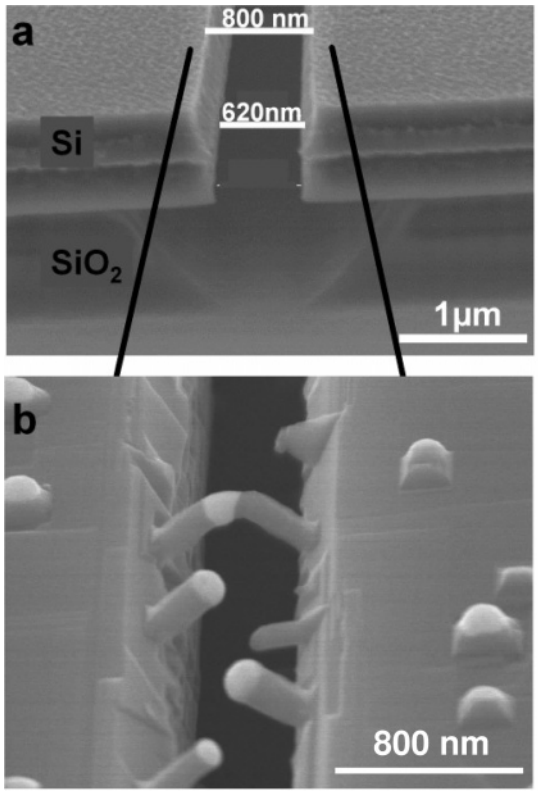

Figure 2. (a) Trench of 600−800 nm width in an SOI wafer after electron beam lithography (EBL) and subsequent reactive ion etching (RIE) using alternative cycles consisting of SF_6/C_4F_8 gas plasmas. (b) VLS growth of silicon NWs from adjacent side walls of the trenches to the middle of the trench after gold layer deposition, subsequent annealing, and MBE growth of silicon NWs.

3. The Raman Signal Enhancement Obtained from Gold Droplets atop Si Nanowires. To measure the signal enhancement produced by only a few (2−3) or even single gold droplets (for the enhancement produced by a single gold droplet see also ref 19) located atop Si NWs, we utilized nanopatterning and self-organized "bottom up" NW growth, as shown in Figure 2. At first, electron beam lithography (EBL) was used to create nanopatterns (here lines) in a resist. The patterns were transferred in a second step by reactive ion etching (RIE) into the top layer of silicon in a silicon-on-insulator (SOI) substrate. Trenches were realized in silicon parallel to the ⟨110⟩ crystallographic direction with widths of 600−800 nm. Then the remaining resist was stripped by an O_2 plasma, and after a subsequent HF treatment (to underetch the SiO_2 layer), the sample was mounted in an MBE UHV chamber for a high-temperature surface cleaning and oxide removal (at 820 °C for 20 min). A gold layer of ∼2 nm thickness was deposited onto the Si(100) surface of the SOI wafer by MBE at 525 °C. Upon annealing at growth temperature, the gold layer desintegrates into droplets on the wafer surface and on the adjacent side walls in the trench. Using MBE Si deposition, nanowires grow from gold droplets only into the ⟨111⟩ directions, i.e., from adjacent sidewalls to the middle of the trench. There they can either meet or, often, gold droplets stay in close proximity without ever impinging. Some impinged and separated nanowires are shown in the SEM micrograph in Figure 2b. These NWs

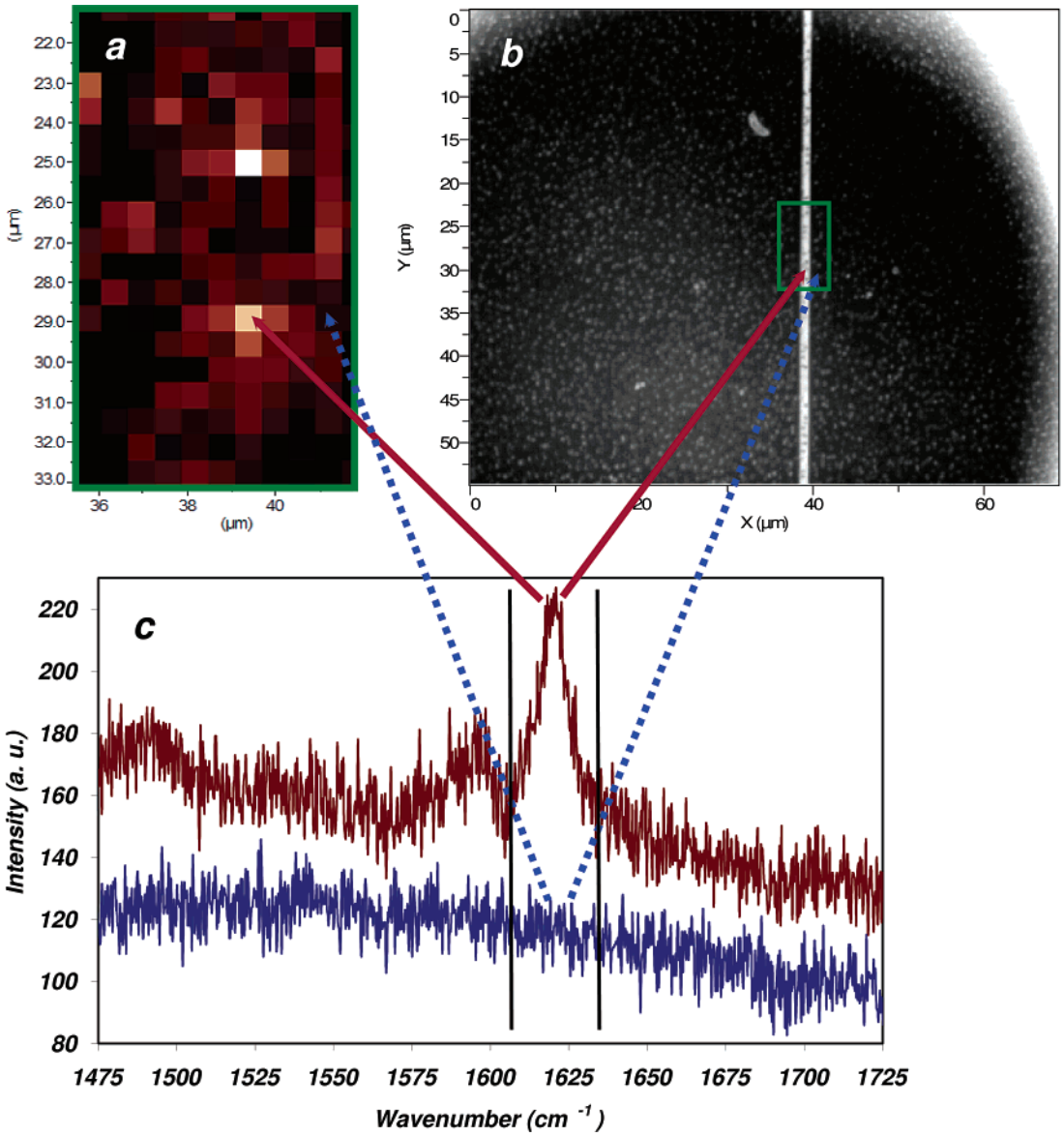

Figure 3. (a) 6 × 12 μm^2 Raman mapped area (indicated by the green box in (a) and (b)). False color coding shows an intensity map of the Raman peak between 1610 cm^{-1}and 1630 cm^{-1} (black lines). Black/dark-brown pixels indicate a weak or no Raman signal, and white/orange show highest Raman intensities. The peak is part of the Raman signature of the malachite green molecule. (b) Light optical micrograph of the SOI substrate with the trench. Gold droplets residing on the substrate are discernible as small whitish spots. The NWs growing within the trench (white) parallel to the ⟨111⟩ directions are visible as small gray lines. (c) Raman spectra within the range of 1475−1725 cm^{-1} acquired at the indicated positions. Highest intensities of the peak between 1610 and 1630 cm^{-1} (see white/orange areas in (a)) occur in places where several gold droplets of NWs reside in close vicinity. To some extent, the gold droplets grown on the substrate surface produce some signal enhancement (dark-red/brown colored positions in (a)). Only fluorescence of malachite green is observed at positions where no gold droplets are present (blue spectrum in (c)).

grew along ⟨111⟩ directions, and they are therefore oblique to the Si(100) surface by an angle of ∼53.7°.

This trench-guided NW assembly was used for SERS measurements. A molecular layer of malachite green was used to study the signal enhancement induced by single gold droplets and configurations of two or more gold droplets on NWs in close proximity. To obtain such a molecular coverage, the samples were rinsed in an aqueous solution of malachite green and subsequently rinsed in deionized water. Afterward, a mapping of the integrated intensity (in between the two black lines in Figure 3c) of the ∼1620 cm^{-1} Raman band of malachite green (in phase stretching of the phenyl rings)[20,21] was performed. During the mapping, the position of the objective and the laser focus stayed fixed. The sample underneath was moved by an automatically controlled $x-y$ stage. For the mapping of the Raman intensities, 12 × 24 measurement points and a step size of 0.5 μm were used. To increase the contrast of the mapping, the broad floures-cence band was substracted. Figure 3 shows the results of the SERS measurements of malachite green on the trench-guided NW configurations of Figure 2. The measurements were carried out with the 633 nm emission line of a He−Ne laser that has an undamped power on the sample of about 10 mW. For the measurements, the laserpower was damped by a factor of 100 to reduce photobleaching of the molecules. With a 100× objective (numerical aperture: 0.9), the laser

could be focused to a spot of about 1 μm in diameter on the sample surface, so that the energy density was about 6×10^3 W/cm^2. The polarization direction of the incident laser beam was chosen perpendicular to the trench. The integration time for one spectrum was 20 s. To reduce the measurement time of the Raman intensity mapping, only the spectral region of malachite green within the range of 1475−1725 cm^{-1} (containing the ∼1620 cm^{-1} band) was acquired.

In most parts of the mapped area (green rectangle in Figure 3a,b), fluorescence but no Raman intensity is visible (as it is color-coded with black in Figure 3a) and demonstrated by the blue spectrum in Figure 3c). Significant signal enhancement occurs at white/orange color-coded positions (red spectrum in Figure 3c). Two white spots indicating large enhancement of the ∼1620 cm^{-1} band arise somewhere close to the middle of the trench where one or more nanowire gold droplets reside (visible as faint gray lines in the optical micrograph in Figure 3b). To some extent, enhancement occurs also at locations (orange/brown) on the Si(100) substrate surface away from the trench. Those spots also correspond to gold droplets (see Figure 2b). The reason for the smaller enhancement on these droplets compared to the ones in the trench could be that the polarization directions of the incident laser beam with respect to the NW axis are different for the different NW orientations. Gold droplets atop NWs grown within the trench experience a polarization vector with a large component parallel to the NW axis. With this configuration, the enhancement is at maximum.[22] This polarization configuration cannot be adopted to the Au droplets grown on the Si(100) surface. There, the polarization direction is mainly perpendicular to the growth axes, and the largest field enhancement is not produced at the top of the gold droplets.

Further signal enhancement could be achieved if two opposing NWs, growing from adjacent sidewalls of the trench, are brought into close proximity (a few nm distance of the two gold droplets). For this purpose, the NW growth conditions and growth times have to be carefully determined. The positions for the NW growth could furthermore be predefined by a localized gold deposition using a focused electron beam (FEB).[23] A large number of such predefined adjacent growth positions and a carefully chosen growth time will allow finding of some of these trench-guided configurations where two droplets reside in close proximity after NW growth within such a trench.

4. A Nanowire Gold Droplet Used as a TERS Probe. Tip-enhanced Raman spectroscopy (TERS) measurements[14,24] can be performed when a Si NW with a gold droplet atop is attached to a standard AFM tip. The attachment can be achieved using a self-made AFM operated in a scanning electron microscopy (SEM) chamber[25] as follows: (1) By ultrasonic treatment, we produce NWs that break off the substrate and fall onto it. (2) The NW substrate is then transferred into the SEM chamber, where we can observe detached NWs. (3) With the AFM tip, the NW can be aligned. (4) With the focused electron beam of the SEM, the Si NW can be welded onto the AFM tip by the deposition of carbonaceous species that reside in the residual gas in the SEM chamber. The SEM micrograph in Figure 4a) shows a silicon NW attached to an AFM tip (short: NW tip) by the welding procedure described above. A magnified SEM micrograph of the tip region is shown in Figure 4b).

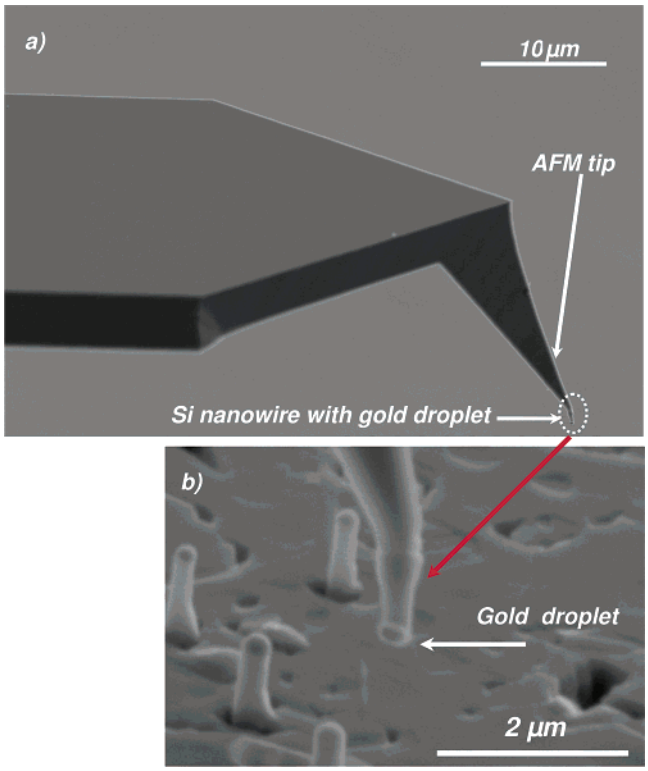

Figure 4. (a) AFM tip with the attached Si nanowire (NW tip). With the focused electron beam in an SEM, the Si NW can be welded onto the AFM tip by the deposition of carbonaceous species. (b) This shows the magnified NW tip region with the attached nanowire. The gold droplet of the Si nanowire is clearly visible.

For our TERS measurements, the NW tips are transferred from the self-made AFM operating in the SEM to a combined AFM Raman spectrometer, where the AFM operates in contact mode and in ambient conditions. A gold-coated standard AFM tip was rinsed with an aqueous solution of malachite green. We refer to this AFM tip as the sample tip. The gold-coated sample tip itself gives rise to a tip-enhanced Raman signal. The NW tip (not contaminated with malachite green) then approaches the gold-coated sample tip from above. The experimental setup is schematically drawn in Figure 5. When the gold droplet of the Si NW is in contact with the sample tip, the Raman signal is expected to be enhanced even more strongly. For largest enhancement, the polarization vector of the incident laser beam should possess a large component along the tip axes,[8] as also illustrated in Figure 5.

We chose this kind of setup mainly for the following reason: As the diameter of the gold droplet is rather small, the tip-enhanced Raman signal of flat samples, such as silicon or synthetic samples, might be obscured to some extent by the background signal.[26] As there is almost no background signal in the spectrum if the inclined incident laser beam is focused onto the outmost end of AFM tips, the additional enhancement produced by the gold droplet of the NW tip can be observed more easily.

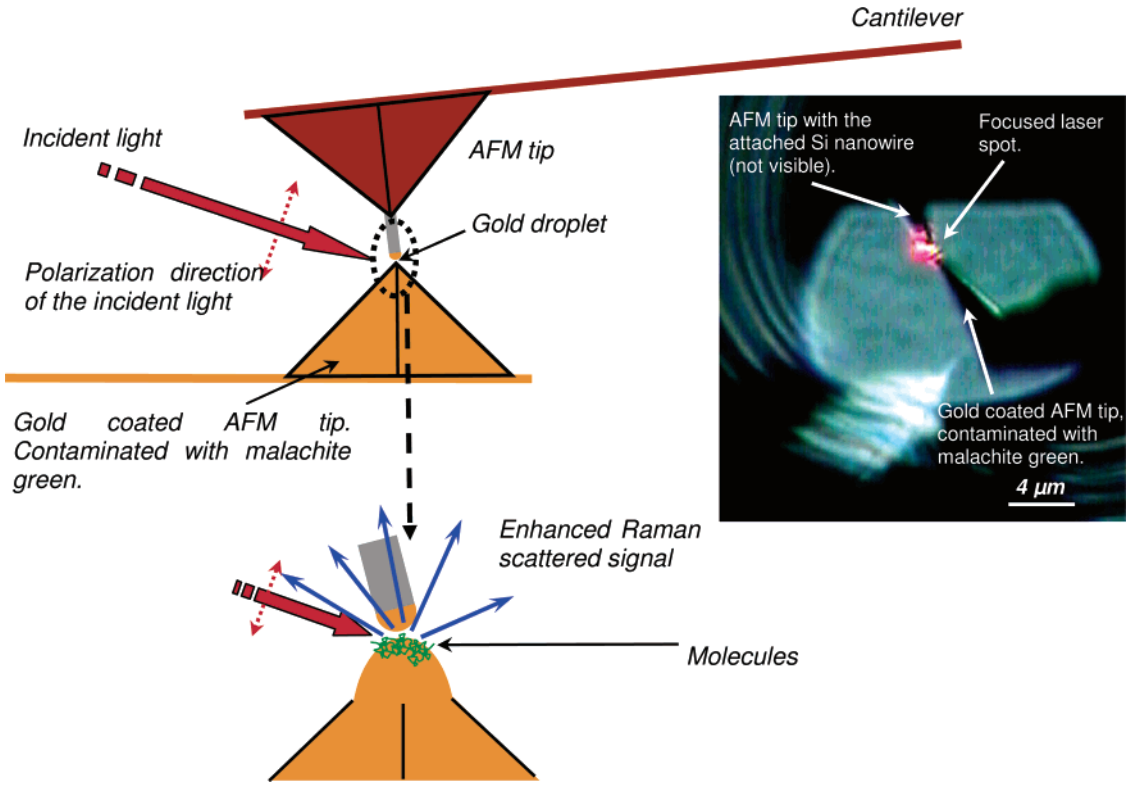

Figure 5. Setup for our TERS measurements with the Si nanowire AFM tip. The AFM tip attached with the Si nanowire with the gold droplet atop is brought close (a few nanometers distance) to a second gold-coated AFM tip (referred to as the sample tip), which is contaminated with malachite green. The sample tip itself produces a tip-enhanced Raman signal due to the gold coating. The gold droplet of the NW tip and the gold-coated sample tip then are in close proximity, and the additional enhancement of the Raman scattered signal due to the gold droplet of the NW tip can be observed. The light optical micrograph shows an inclined side view of the experimental setup. Both tips and the position of the focused laser spot are visible.

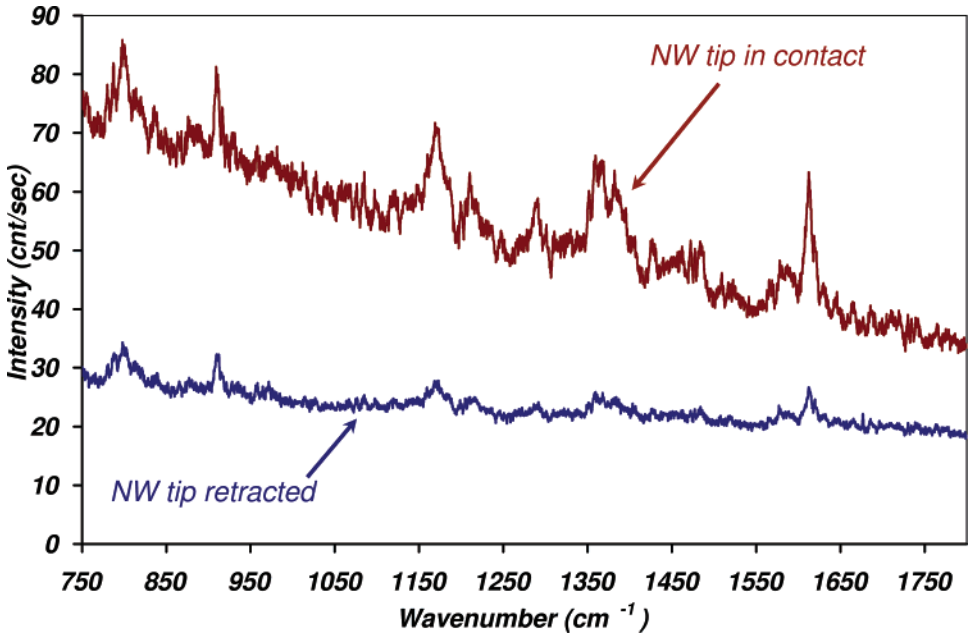

Figure 6. Enhanced Raman spectra of malachite green between 750 and 1750 cm^{-1}. The blue spectrum of malachite green shows the signal enhancement solely produced by the gold-coated sample tip. When the NW tip is in contact with the sample tip, the enhancement becomes 6−7 times larger (red spectrum).

The disadvantage of the setup is the tedious alignment of the two adjacent AFM tips. The light optical micrograph in Figure 5 shows an inclined view of the setup. The cantilever with the NW tip resides on top of the cantlilever with the gold-coated sample tip. The He−Ne (633 nm) laser of the Raman spectroscometer (Jobin Yvon LabRam HR 800) is focused onto both tip ends and its polarization direction is mainly along the tip axes.

With the nanowire tip in contact with the gold-coated sample tip, a Raman spectrum was acquired using 0.1 mW laser power and an integration time of 30 s. Then the NW tip was retracted and a second spectrum was acquired with the laser spot at the same position but now only hitting the end of the sample tip. The same laser power but an integration time of 60 s was then used. The longer integration time improves the signal-to-noise ratio but has no effect on the signal intensity if counts/s are aquired. The resulting spectra within the range of 750−1750 cm^{-1} are shown in Figure 6. The gold-coated sample tip itself produces a tip-enhanced Raman signal of malachite green (blue spectrum). But with the NW tip in contact with the sample tip, additional enhancement is achieved (red spectrum). In the case of a contact to the sample tip, the observed enhancement of the Raman signal becomes 6−7 times larger than with the NW tip retracted.

5. Conclusion. We showed that hemispherical gold droplets atop silicon nanowires grown by the VLS mechanism produce significant enhancement of Raman scattered signals. A probe for tip-enhanced Raman spectroscopy (TERS) measurements was fabricated by welding a silicon nanowire with a gold droplet atop onto an AFM tip. This TERS tip has the potential to be used in Raman spectroscopy with a nanoscale spatial resolution. A configuration where the NW tip and the gold-coated AFM tip were in close proximity was established. By using this configuration, the additional enhancement produced solely by the single gold droplet on top of a silicon nanowire was measured. The observed enhancement of the Raman scattered signal of malachite green, with the nanowire gold droplet in contact with the gold-coated AFM tip, was 6−7 times larger than the tip enhancement produced solely by the gold-coated AFM tip. The signal enhancement produced by gold droplets atop silicon nanowires could be further improved by: (i) using smaller nanowires with smaller gold droplets, (ii) improving the aligning and approaching routines of the coupled AFM Raman spectrometer setup to optimize the configuration formed by the two tips, and (iii) using either two NW tips in contact or a NW on a substrate in contact with a NW tip.

Strong enhancement could also be achieved by configurations formed by two gold droplets atop Si NWs in close proximity that are grown on adjacent side walls of a trench which is etched into a silicon wafer. To produce such a configuration, the growth positions of nanowires have to be predefined and growth times have to be carefully selected. Predefined positioning of gold droplets could be achieved by gold deposition using a focused electron beam. The preliminary results of these experiments are promising, and we will report on SERS measurements using these trench-guided nanowire configurations within a short time.

Acknowledgment. S. Christiansen acknowledges the financial support by the German Science Foundation (DFG) under contract number CH-159/1 and by the excellence initiative of the Land of Saxony-Anhalt, Germany. S. Hoffmann acknowledges the Swiss National Science Foundation for financial support. We especially acknowledge H. P. Strunk (Institute of Microcharacterization, University Erlangen-Nuremberg) for providing the micro-Raman spectroscope and the Nanoworld AG, Switzerland, for providing the AFM tips. We would like to thank H. Stafast for providing the necessary infrastructure to carry out the EBE growth experiments and A. Assmann for carrying out some scanning electron microscopy (both IPHT, Jena/Germany). G. Brehm, G. Sauer (Department of Physical and Theoretical Chemistry, University Erlangen-Nuremberg) F. Falk, Th. Stelzner (IPHT, Jena/Germany) and H. J. Reich (Horiba Jobin Yvon SAS, France) are greatfully acknowledged for fruitful discussions.

References

(1) Fleischmann, M.; Hendra, P. J.; McQuillan, A. J. *Chem. Phys. Lett.* **1974**, *26*, 163.
(2) Albrecht, M. G.; Creighton, J. A. *J. Am. Chem. Soc.* **1977**, *99*, 5215.
(3) Jeanmarie, D. L.; Van Duyne, R. P. *J. Electroanal. Chem.* **1977**, *84*, 1.
(4) Kneipp, K.; Kneipp, H.; Itzkan, I.; Dasari, R. R.; Feld, M. S.; Dresselhaus, M. S. *Top. Appl. Phys.* **2002**, *82*, 227.
(5) Nie, S.; Emory, S. R. *Science* **1997**, *275*, 1102.
(6) Emory, S. R.; Nie, S. *Anal. Chem.* **1997**, *69*, 2631.
(7) Sivakov, V.; Andrä, G.; Himcinschi, C.; Gösele, U.; Zahn, D. R. T.; Christiansen, S. H. *Appl. Phys. A*, accepted for publication.
(8) Moskovits, M. *Rev. Mod. Phys.* **1985**, *57*, 783.
(9) Wagner, R. S.; Ellis, W. C. *Appl. Phys. Lett.* **1964**, *4*, 89.
(10) Givargizov, E. I. *J. Cryst. Growth* **1975**, *31*, 20.
(11) Kalkbrenner, T.; Ramstein, M.; Mlynek, J.; Sandoghdar, V. *J. Microsc.* **2001**, *202*, 72.
(12) Zenhauser, F.; Martin, Y.; Wickramasinghe, H. K. *Science* **1995**, *269*, 1083.
(13) Aigouy, L.; Larech, A.; Gresillon, S.; Cory, H.; Boccara, A. C.; Rivoal, J. C. *Opt. Lett.* **1999**, *24*, 187.
(14) Stöckle, R. M.; Sun, Y. D.; Deckert, V.; Zenobi, R. *Chem. Phys. Lett.* **2000**, *318*, 131.
(15) Fischer, U. C.; Pohl, D. W. *Phys. Rev. Lett.* **1989**, *62*, 458.
(16) Civale, Y.; Nanver, L. K.; Hadley, P.; Goudena, E. J. G. *Proc. SAFE Conf.* **2004**, 692.
(17) Ostwald, W. *Z. Phys. Chem.* **1901**, *37*, 385.
(18) Ostwald, W. *Analytisch Chemie*, 3rd ed.; Engelmann: Leipzig, 1901; p 23.
(19) Becker, M.; Sivakov, V.; Gösele, U.; Andrä, G.; Reich, H. J.; Hoffmann, S.; Michler, J.; Christiansen, S. H. *Small*, submitted.
(20) Schneider, S.; Brehm, G.; Freunscht, P. *Phys. Status Solidi B* **1995**, *189*, 37.
(21) Doering, W. E.; Nie, S. M. *Anal. Chem.* **2003**, *75*, 6171.
(22) Moskovits, M. *J. Raman Spectrosc.* **2005**, *36*, 485.
(23) Utke, I.; Luisier, A.; Hoffmann, P.; Laub, D.; Buffat, P. A. *Appl. Phys. Lett.* **2002**, *81*, 3245.
(24) Pettinger, B.; Ren, B.; Picardi, G.; Schuster, R.; Ertl, G. *Phys. Rev. Lett.* **2004**, *92*, 096101-1.
(25) Hoffmann, S.; Utke, I.; Moser, B.; Michler, J.; Christiansen, S.; Schmidt, V.; Senz, S.; Werner, P.; Gösele, U.; Ballif, C. *Nano Lett.* **2006**, *6*, 622.
(26) Mehtani, D.; Lee, N.; Hartschuh, R. D.; Kisliuk, A.; Foster, M. D.; Sokolov, A. P.; Maguire, J. F. *J. Raman Spectrosc.* **2005**, *36*, 1068.

NL0621286